

Anharmonic analysis of the vibrational spectrum of ketene by density functional theory using second-order perturbative approach

V.P. Gupta*

Department of Physics, University of Jammu, Jammu-Tawi 180006, India

Received 5 July 2006; received in revised form 24 August 2006; accepted 1 September 2006

Abstract

The paper reports main results of a comprehensive study of the vibrational spectrum of ketene computed using second-order perturbation theory treatment based on quartic, cubic and semidiagonal quartic force constants. Two different models – a homogeneous model using the same density functionals and basis functions for the harmonic calculations and anharmonic corrections and a hybrid model in which the two parts of the calculation are conducted using different density functionals and basis sets – have been employed in the present calculations. Different DFT and CCSD methods and DZ and TZ extended basis sets involving diffuse and polarization functions have been used to calculate optimized and vibrationally averaged geometrical parameters, the harmonic and anharmonic vibrational frequencies and the spectroscopic constants such as anharmonicity constants, rotational constants, rotation–vibration coupling constants, Nielsen’s centrifugal distortion constants and Coriolis coupling constants. Homogeneous model is found to be superior to the hybrid model in several respects. Difficulties in the hybrid model may arise due to one of the following reasons: (a) the basic requirement that the geometry optimization and frequency calculations must be done at the same level of theory to have valid frequencies is not met in the hybrid model; (b) the molecular structure gets reoptimized at the low level for anharmonic corrections; (c) in addition, the perturbation could also diverge for the above reasons, particularly for the very low, very anharmonic terms where the harmonic approximation is not close enough to make the perturbation work.

© 2006 Published by Elsevier B.V.

Keywords: Ketene; DFT; Anharmonic frequencies; Coupling constants; Fundamental bands; Overtones; Combination bands

1. Introduction

Computation of harmonic force fields by quantum chemical methods has provided an invaluable aid in the assignment of spectra, specially for the unstable molecular species. However, introduction of suitable scaling factors is unavoidable at this level due both to the quantum chemical models and neglect of anharmonicity. In this context, second-order perturbative theory, which provides closed expressions for most of the spectroscopic parameters required for the analysis of the experimental frequencies, appears to be very effective for the study of polyatomic molecules of medium dimensions [1–6]. Boese and Martin [4] have assessed the performance of modern density functional theory (in particular, B97-1/TZ2P) for the anharmonic vibrational analysis of azabenzenes and have concluded that quartic force fields combined with second-order rovibrational pertur-

bation theory show promise for the assignment of vibrational spectra of medium sized organic molecules. In a similar study, Barone [7] has suggested that best results can be obtained by using a hybrid model in which the harmonic frequency calculations using hybrid functionals (B3LYP/B97-1/B97-2, etc.) and large basis sets are combined with anharmonic corrections using less expensive method B3LYP/6-31+G*. We have earlier reported results of anharmonic vibrational analysis of some cyanides and related molecules of astrophysical significance [8] using both the MP2 and DFT methods. In order to verify the suggestion of Barone [7] in the use of hybrid model for anharmonic analysis, we have extended our studies to an unstable molecule ketene for which a large amount of literature related to experimental and theoretical studies on the structure [9,10] and harmonic and anharmonic analysis of the vibrational spectra [11–14] is available. Second-order perturbative approach within the framework of the density functional theory was employed to calculate harmonic and anharmonic frequencies and spectroscopic constants such as rotational and rotational–vibrational constants, distortion and coupling con-

* Tel.: +91 191 2453079; fax: +91 191 2453079.
E-mail address: vpopt1@yahoo.co.in.

stants, etc. Both the hybrid model, as suggested by Barone [7] and the usual homogeneous model in which the harmonic frequencies and the anharmonic corrections are calculated by the same methods and basis sets, have been used in the present study.

2. Methodology

The potential energy function for an anharmonic oscillator may be written as:

$$V = \frac{1}{2} \sum_{ij} f_{ij} S_i S_j + \frac{1}{6} \sum_{ijk} f_{ijk} S_i S_j S_k + \frac{1}{24} \sum_{ijkl} f_{ijkl} S_i S_j S_k S_l + \dots \quad (1)$$

$\{S_i\}$ represent a displacement internal coordinate and $f_{ij}, f_{ijk}, f_{ijkl}$, etc. are the quadratic, cubic and quartic, etc. force constants. Using the Dunham potential functions, the energy of an anharmonic oscillator is given by:

$$E_{n_1, n_2, \dots} = \sum_i v_{0i} \left(n_i + \frac{1}{2} \right) + \sum_{\substack{i, k \\ k \geq 1}} X_{ik} \left(n_i + \frac{1}{2} \right) \left(n_k + \frac{1}{2} \right) + \dots \quad (2)$$

where X_{ii} and X_{ik} are the diagonal and non-diagonal anharmonicity constants. While X_{ii} characterizes anharmonicity of the given vibration, the coefficients X_{ik} characterizes coupling between different normal modes resulting from anharmonicity and are determined from cubic and quartic force constants. The funda-

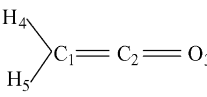
mental frequencies of the anharmonic oscillator are given by:

$$\nu'_i = \nu_{0i} + 2X_{ii} + \frac{1}{2} \sum_{j \neq i} X_{ij} \quad (3)$$

The rotational–vibrational couplings are determined in terms of the rotational, centrifugal distortion and rotation–vibration interaction constants and Coriolis coupling coefficients.

The anharmonic force fields and spectroscopic constants have been calculated by using the second-order perturbation theory (PT2) implemented in the G03W [15] software. The calculations were conducted using B3LYP, B97-1 and CCSD procedures with 6-31+G**, 6-311++G(2df,2p) and aug-cc-pVTZ basis sets involving diffuse functions and polarization functions. Anharmonic corrections using PT2 were carried out by employing: (a) the same method and basis set as used in the harmonic calculations (homogeneous model) and (b) different methods and basis sets than used in the harmonic calculations (hybrid model). This latter procedure was used to verify the findings of Barone [7] that the best results for anharmonic analysis are obtained by employing mixed methods (hybrid model). It has been shown in our earlier publication [8] that not only in the harmonic but also in the anharmonic approximations, the calculated frequencies from extended basis RHF and MP2 methods are much higher than the experimental frequencies and need scaling in both the cases. In contrast, the DFT frequencies in the two approximations are much closer to the experimental frequencies and the scaling is needed only in the harmonic approximation. It was found that the anharmonic frequencies using DFT do not need further scaling and match with the experimental values within $\pm 18 \text{ cm}^{-1}$ on an average. As such, in the present computations, only the density functional and coupled cluster (CCSD) theories have been employed. The forms of vibrations were analyzed using the software GaussView W version 2.0 [16].

Table 1

Optimized and vibrationally averaged molecular geometries, dipole moment and total energy of ketene 								
Bond length/ bond angle	Experimental values ^a	Ref. [14] (optimized)	B97-1/aug-cc-pVTZ//B97-1/ aug-cc-pVTZ		B97-1/6-311++G**// B97-1/6-311++G**		B3LYP/6-31+G**// B3LYP/6-31+G**	
			Optimized	Averaged ^b	Optimized	Averaged	Optimized	Averaged
C ₁ =C ₂	1.314 ± 0.010	1.3142	1.3116	1.3153	1.3136	1.3173	1.3165	1.3201
C ₂ =O ₃	1.161 ± 0.010	1.1609	1.1613	1.1627	1.1621	1.1636	1.1712	1.1726
C ₁ –H ₄	1.083 ± 0.002	1.0753	1.0800	1.0825	1.0819	1.0844	1.0825	1.0854
C ₁ –H ₅	1.083 ± 0.002	1.0753	1.0800	1.0825	1.0819	1.0845	1.0825	1.0855
C ₁ C ₂ O ₃	–	180.00	180.00	180.00	179.95	179.96	179.98	179.98
H ₄ C ₁ C ₂	–	–	119.42	119.22	119.69	119.50	119.71	119.51
H ₅ C ₁ C ₂	–	–	119.42	119.22	119.68	119.49	119.70	119.50
H ₄ C ₁ H ₅	122.6 ± 0.3	121.76	121.15	121.57	120.68	121.06	120.61	121.02
H ₅ C ₁ C ₂ O ₃	0.0	0.0	0.0	0.0	0.0	0.0	0.0	0.0
Dipole moment	1.414 ^c	–	1.4939	–	1.5333	–	1.6101	–
Energy (a.u.)	–	–	–152.6160790	–	–152.6024003	–	–152.6109023	–

^a Vibrationally averaged parameters at 0 K.

^b Ref. [26].

^c Ref. [29].

3. Results and discussion

A review of the infrared and microwave spectral studies on ketene over the last six decades has been given by East et al. [14]. Infrared work on gaseous ketene and its deuterated variants which achieved partial resolution of rotational band contours, in conjunction with the microwave data, provided tentative assignments for numerous overtone and combination levels [11,14,17]. East et al. [14] carried out a comprehensive anharmonic vibrational analysis of isotopic ketenes on the basis of a complete *ab initio* quartic force field constructed by MP2 and CCSD approach followed by iterative anharmonic vibrational refinement of a limited set of quadratic scaling parameters and reported a complete and self-consistent set of Coriolis, vibrational anharmonic, vibration–rotation interaction and centrifugal distortion constants and molecular geometries. No similar study based on density functional theory and using the second-order perturbational approach is available for ketene. Results of our calculations for ketene based on different DFT and CCSD methods and DZ and TZ extended basis sets involving diffuse and polarization functions are given in Tables 1–6. The optimized and vibrationally averaged geometrical parameters, the harmonic and anharmonic vibrational frequencies and the spectroscopic constants such as anharmonicity constants, rotational constants, rotation–vibration coupling constants, Nielsen’s centrifugal distortion constants and Coriolis coupling constants of ketene are being presented and discussed separately. A reasonable agreement with the experimental frequencies has, in general, been obtained in cases where the calculations were conducted using the homogeneous model within the DFT and CCSD framework. Larger deviations are, however, found for the higher frequency CCO asymmetric stretch mode. Boese and Martin [4] trace the larger errors in high frequency modes in their DFT-based calculations to finite difference step-sizes. In the present calculations, a step-size of 0.025 Å has been used in the anharmonic calculations.

3.1. Molecular geometry

The optimized and vibrationally averaged molecular geometry, dipole moment and total energy of ketene by the homogeneous model using B97-1/aug-cc-pVTZ, B97-1/6-311++G* and B3LYP/6-31+G** methods are given in Table 1. The table also contains experimental [18] and theoretical [14] values of bond lengths and bond angles given in the literature. It follows from this table that the optimized bond lengths and bond angles of ketene are in good agreement with the experimental values reported by Cox et al. [18], within the error limits, and the CCSD/QZ(2d,2p)-based theoretical values of East et al. [14] involving diatomic model for bond anharmonicity and appropriate Morse anharmonicity parameters. The vibrationally averaged bond lengths are longer than the optimized lengths by 0.001–0.003 Å but the averaged bond angles are shorter than the optimized bond angles by about 0.2°.

Table 2
Vibrational frequencies (cm^{-1}), intensities (km/mol) and assignments of ketene

Frequencies	Experimental	B97-1/aug-cc-pvtz// B3LYP/6-31+G**				B97-1/aug-cc-pvtz// B97-1/6-311++G**				B97-1/6-311++G**// B3LYP/6-311++G**				B3LYP/6-31+G**// B3LYP/6-31+G**				Assignments
		Harmonic		Anharmonic (ν_{calc})		Harmonic		Anharmonic (ν_{calc})		Harmonic		Anharmonic (ν_{calc})		Harmonic		Anharmonic (ν_{calc})		
		ν_{calc}		Intensities		ν_{calc}		Intensities		ν_{calc}		Intensities		ν_{calc}		Intensities		
Symmetry A_1																		
	ν_1	3070	3220.4	29.0	3086.9	3174.1	27.6	3072.2	3175.5	30.5	3031.6	3177.5	29.9	3047.4	3177.5	28.9	3063.7	CH symmetric stretch
	ν_2	2151	2279.9	673.8	2237.2	2213.6	670.3	2173.0	2226.8	682.6	2185.6	2223.4	693.1	2180.3	2223.4	660.6	2170.3	CCO asymmetric stretch
	ν_3	1388	1419.5	18.3	1392.9	1404.2	20.5	1375.8	1399.6	19.6	1372.6	1406.0	18.4	1378.7	1406.0	17.5	1388.6	CCH i.p. bend
																		CCO symmetric stretch
	ν_4	1117.8	1187.2	6.3	1200.4	1166.9	4.2	1119.3	1166.7	5.8	1115.2	1170.8	6.6	1139.8	1170.8	6.7	1133.8	
Symmetry B_1																		
	ν_5	588	574.6	125.5	568.5	586.6	11.0	577.4	594.7	87.9	576.6	600.8	107.9	587.6	600.8	122.9	593.5	CCH o.p. bend
	ν_6	528	507.5	33.7	508.1	535.1	1.6	530.2	544.3	56.5	533.6	554.9	34.0	550.5	554.9	34.3	531.9	CCO o.p. bend
Symmetry B_2																		
	ν_7	3166	3318.6	9.51	3169.3	3270.3	9.6	3164.7	3272.2	11.0	3111.8	3270.6	9.7	3124.8	3270.6	9.4	3142.3	CH asymmetric stretch
	ν_8	976.7	984.1	9.27	968.6	986.7	8.8	971.2	984.9	7.7	969.4	987.0	8.0	971.2	987.0	9.0	975.2	CCH i.p. bend
	ν_9	438	404.0	2.76	402.8	442.1	2.8	441.2	441.9	2.1	440.0	443.7	2.2	441.3	443.7	2.6	436.8	CCO i.p. bend

The two methods indicated in the table refer to harmonic frequencies and anharmonic corrections, respectively.

3.2. Harmonic and anharmonic fundamental modes

Two types of calculations were performed to obtain the frequencies and intensities of the fundamental modes and the overtones and combination bands. In the first case, the usual homogeneous model was adopted and both the harmonic frequencies and the anharmonicity corrections were calculated by using the same method and basis set viz. B3LYP/6-31+G**, B3LYP/6-311++G**, B97-1/6-311++G** and B97-1/aug-cc-pVTZ. In the second case, the calculations were conducted using a hybrid model: the harmonic calculations were conducted using DFT(B97-1) and CCSD methods with large basis sets and the anharmonic corrections by DFT(B3LYP) method and relatively small basis sets. These calculations were conducted using CCSD/6-311+G**/B3LYP/6-31+G** and B97-1/aug-cc-pVTZ/B3LYP/6-31+G** methods. The results of some of these calculations together with the experimental frequencies are given in Table 2.

It may be seen that the calculated harmonic frequencies need significant scaling for agreement with the experimental values. No such scaling is needed for the anharmonic frequencies which are quite close to the experimental values. However, while in the homogeneous model, the average agreement between the calculated anharmonic frequencies and experimental frequencies is 10 cm^{-1} , in the hybrid model it is 30 cm^{-1} . Also, the maximum deviation from the experimental values in the first case is much lower than in the second case. It is also observed that the anharmonic corrections to the frequencies in the homogeneous model is uniformly negative where as in the hybrid model it may also be positive as in the case of frequencies ν_4 and ν_6 .

3.3. Overtones and combination bands

Based on infrared and microwave data, well over 2000 overtones and combination bands for isotopic ketenes have been

catalogued [14] many of which are yet to be confirmed or reanalyzed in high resolution. It has been noted by Johns et al. [19] that vibrational bands of ketene suffer severe perturbations mainly because of the presence of low lying vibrational states ($\nu_5 = 587\text{ cm}^{-1}$, $\nu_6 = 520\text{ cm}^{-1}$, $\nu_9 = 439\text{ cm}^{-1}$) whose overtones and combination bands are scattered over the mid-infrared region and give rise to Fermi and Coriolis interactions. Some of the selected overtone and combination tone bands from the present calculations using the homogeneous and hybrid models together with their experimental values are given in Table 3. A comparison of these calculated values by B3LYP/6-31+G**, B97-1/6-311++G** and B97-1/aug-cc-pVTZ methods using the homogeneous model with the experimental values [9,11,17,20–22], and the calculated values of East et al. [14] by QZ(2d,2p) SQM(CCSD)+MP2/EXPT anharmonic force field shows that the results are in reasonable agreement with each other. Present calculations with homogeneous model B97-1/aug-cc-pVTZ predict a strong Fermi resonance between frequencies ν_4 and $2\nu_5$ separated by about 6 cm^{-1} , as also suggested by East et al. [14], and give their deperturbed values at 1119.3 and 1184.4 cm^{-1} , respectively. However, Fermi resonance between ν_4 and $2\nu_6$, which are separated by $\sim 100\text{ cm}^{-1}$, could not be confirmed. The calculations also do not show any significant Coriolis interaction between ν_4 and ν_6 (Table 5). In contrast, the hybrid model suggested by Barone [7] fails to predict Fermi resonance between ν_4 and $2\nu_5$.

Present calculations also predict a combination band $\nu_6 + \nu_9$ at 976.8 cm^{-1} near the experimental ν_8 band at 977.8 cm^{-1} . Z-components of the Coriolis interaction interaction constants $Z(8, 6) = -0.7327$ and $Z(9, 6) = -0.4074$ also suggest a strong Coriolis interaction between these bands. The experimental observation of the $\nu_6 + \nu_9$ band of ketene via resonant Coriolis interaction with ν_8 in $940\text{--}970\text{ cm}^{-1}$ region by Gruebele et al. [17], confirms the present theoretical prediction. It is also observed that the calculated frequencies of overtones and combi-

Table 3
Overtones and combination tones (cm^{-1}) of ketene and their assignments

Experimental	Calculated								Assignments
	B3LYP/6-31+G**// B3LYP/6-31+G**		B97-1/6-311++G**// B97-1/6-311++G**		B97-1/aug-cc-pVTZ// B97-1/aug-cc-pVTZ		B97-1/aug-cc-pVTZ// B3LYP/6-31+G**		
	Harmonic	Anharmonic	Harmonic	Anharmonic	Harmonic	Anharmonic	Harmonic	Anharmonic	
–	4426.0	4318.9	4452.9	4349.8	4427.3	4325.9	4559.1	4452.0	2ν ₂
1952.4 ^a , 1947 ^b	1981.3	1947.6	1972.3	1939.7	1973.5	1940.2	1968.8	1935.1	2ν ₈
–	1182.9	1191.1	1173.1	1184.5	1173.1	1184.4	1149.4	1110.2	2ν ₅
–	1062.8	1059.7	1088.4	1059.2	1070.2	1064.9	1015.9	1014.2	2ν ₆
6113.3 ^c	6491.6	6085.3	6449.7	6015.9	6444.5	5990.8	6537.5	6134.6	ν ₁ + ν ₇
3513.0 ^b	3629.1	3552.9	3625.2	3551.3	3617.8	3543.1	3699.3	3623.2	ν ₂ + ν ₃
3255 ^b , 3266.0 ^d	3383.6	3291.9	3392.4	3272.3	3380.6	3313.1	3467.1	3425.7	ν ₂ + ν ₄
3126.7 ^e	3203.7	3139.5	3212.6	3147.9	3200.4	3136.7	3263.9	3197.5	ν ₂ + ν ₈
2513.6 ^c	2586.6	2518.9	2564.6	2467.9	2751.1	2524.5	2607.3	2590.3	ν ₃ + ν ₄
1126.0 ^b	1131.3	1127.0	1135.6	1097.8	1121.7	1105.3	1082.7	1081.1	ν ₅ + ν ₆
940–970 ^f	969.3	976.8	985.8	976.8	977.2	973.8	912.6	920.2	ν ₆ + ν ₉

^a Ref. [20].

^b Ref. [11].

^c Ref. [21].

^d Ref. [9].

^e Ref. [22].

^f Ref. [17].

Table 4
Anharmonicity constants X_{ij} (cm^{-1}) for ketene

<i>I</i>	<i>J</i>	X_{ij}		
		Method 1 ^a	Method 2 ^b	Ref. [15]
1	1	−31.14	−27.79	−26.66
2	1	−1.89	−1.76	−2.04
2	2	−10.05	−10.58	−11.15
3	1	−5.53	−2.53	−5.70
3	2	−5.69	−6.75	−4.76
3	3	−6.34	−6.54	−6.29
4	1	−4.67	−5.16	−3.85
4	2	−11.68	−11.82	−13.97
4	3	−3.03	−3.59	−2.88
4	4	−1.06	−0.85	−1.15
5	1	−9.03	−11.91	−5.87
5	2	−3.90	−2.61	−4.25
5	3	8.43	9.27	11.12
5	4	−4.04	51.70	−3.78
5	5	−1.41	−13.32	0.28
6	1	−10.39	−3.10	−8.81
6	2	−9.29	−11.11	−9.83
6	3	4.59	1.85	6.78
6	4	−1.03	2.65	−5.53
6	5	−2.33	4.05	14.92
6	6	2.23	−1.45	14.83
7	1	−132.32	−119.88	−112.25
7	2	4.12	−5.11	−0.14
7	3	−17.98	−14.99	−18.42
7	4	−4.35	−5.24	−3.41
7	5	−13.14	−18.60	−10.42
7	6	−15.25	−4.10	−16.05
7	7	−36.18	−32.79	−31.17
8	1	−11.38	−9.63	−9.94
8	2	−7.51	−8.19	−3.28
8	3	−9.94	−9.16	−9.06
8	4	−1.23	−1.49	−1.25
8	5	1.34	4.84	0.45
8	6	12.67	8.52	8.02
8	7	−9.59	−7.04	−12.03
8	8	−1.12	−1.31	−1.83
9	1	−4.52	−2.01	−1.22
9	2	−5.22	−6.00	−5.96
9	3	−2.30	−1.19	−0.86
9	4	3.92	2.84	4.06
9	5	10.05	4.03	10.89
9	6	2.31	8.25	3.76
9	7	−5.16	−2.93	−1.89
9	8	−0.93	−3.64	−1.45
9	9	0.04	−0.43	0.68

^a Homogeneous model B97-1/aug-cc-pVTZ//B-97-1/aug-cc-pVTZ.

^b Hybrid model B97-1/aug-cc-pVTZ//B3LYP/6-31+G**.

nation bands by the homogeneous model are in better agreement with experiment than those from the hybrid model.

3.4. Anharmonicity constants

The anharmonicity constants X_{ij} of ketene from homogeneous model B97-1/aug-cc-pVTZ (method 1) and hybrid model B97-1/aug-cc-pVTZ//B3LYP/6-31+G** (method 2), are given in Table 4. The table also contains, for comparison, the anharmonicity constants computed by East et al. [14] from QZ(2d,2p) SQM(CCSD)+MP2//EXPT anharmonic force field. It is seen

from the table that the anharmonicity constants obtained from the homogeneous model are in closer proximity to literature [14] than those obtained from the hybrid model; large deviations are, however, found for X_{65} and X_{66} . While the diagonal anharmonicity constants for the stretching modes have a negative value in method 1, those corresponding to the group of frequencies ν_5 , ν_6 and ν_9 involving substantial C=C=O deformation either have a very small negative value ($X_{55} = -1.41$) or a small positive value ($X_{66} = 2.23$, $X_{99} = 0.04$). The value of X_{55} in method 2 is -13.32 which may be due to exclusion of (ν_4 , $2\nu_5$) interaction.

3.5. Rotational and rotation–vibration coupling constants

Rotational constants of ketene obtained from different methods and basis sets together with the data of East et al. [14] based on QZ(2d,2p) SQM(CCSD)+MP2//EXPT anharmonic force field and the empirical constants of Johns et al. [13] from S-reduced Hamiltonian are given in Table 5. Moore and Pimentel [11] have compiled rotational constants of ketenes obtained from high-resolution microwave and infrared measurements and suggest that the best available estimate for A_0 is $9.36 \pm 0.02 \text{ cm}^{-1}$. The microwave data [10] gives a value 9.28 cm^{-1} which, as pointed out by Duncan and Munro [23], appears to be in error since only $\Delta K_a = 0$ transitions are strong in near prolate asymmetric rotors like ketene. The present values of rotational constants A_0 , B_0 , C_0 which contain effects due to zero-point vibrations and centrifugal distortion are close to those of East et al. [14]. Both, the homogeneous and hybrid models are found to give similar values for the rotational constants.

The rotation–vibration coupling constants based on the second-order perturbative vibrational treatment using density functional theory are given in Table 5 and compared with the results obtained from QZ(2d,2p) SQM(CCSD)+MP2//EXPT anharmonic force field. It may be seen from this table that there is a close agreement in the values obtained from different methods and basis sets except for the interchange in α_5^a and α_6^a values in some cases. It has been documented [24,25] that there exists a strong Coriolis interaction amongst the ν_5 , ν_6 , ν_8 , ν_9 fundamentals of isotopic ketenes and that for detailed comparison of theory and experiment in such cases, a deperturbation of certain α_i values is needed. Present calculations as well as those of East et al. [14], however, do not show a strong Coriolis interaction between ν_5 and ν_6 (Table 6) and, therefore, cannot explain the interchange in α_5^a and α_6^a values on this basis. The values from the homogeneous model are in better agreement with the literature [14] than those from the hybrid model.

3.6. Coriolis and Nielsen's centrifugal distortion constants

Coriolis coupling coefficients $Z(I, J)$ between the various vibrational modes have been worked out in accordance with Jahn's rule [26]. These are given in Table 6 for different levels of density functional theory calculations using homogeneous and hybrid models and compared with the values of East et al. [14] from QZ(2d,2p) SQM(CCSD)+MP2//EXPT anharmonic force field calculations. The values obtained from the homoge-

Rotational constants (cm^{-1}) including terms due to quartic centrifugal distortion constants and rotational–vibrational coupling constants (cm^{-1}) of ketene

	B3LYP/6-31+G**// B3LYP/6-31+G**	B3LYP/6-311++G**// B3LYP/6-311++G**	B97-1/6-311++G**// B97-1/6-311++G**	B97-1/aug-cc-pVTZ// B97-1/aug-cc-pVTZ	B97-1/aug-cc-pVTZ// B3LYP/6-31+G**	Ref. [14]
Rotational constants						
A_e	9.44966	9.49401	9.43465	9.45155	9.45155	—
B_e	0.33960	0.34394	0.34283	0.34378	0.34378	—
C_e	0.32782	0.33192	0.33081	0.33172	0.33172	—
A_0	9.44966 ^a	9.49400	9.43465	9.45155	9.45155	9.40990
B_0	0.33960	0.34394	0.34283	0.34378	0.34378	0.34335
C_0	0.32781	0.33192	0.33080	0.33172	0.33172	0.33072
	B3LYP/6-31+G**// B3LYP/6-31+G**	B97-1/aug-cc-pVTZ// B97-1/aug-cc-pVTZ		B97-1/aug-cc-pVTZ// B3LYP/6-31+G**	Ref. [14]	
	a b c	a b c		a b c	a b c	
Rotation–vibration coupling constants ($\times 10^{-3} \text{ cm}^{-1}$)						
α_1	159.1	0.27	0.44	159.4	0.27	0.44
α_2	11.8	23.6	2.20	11.3	2.31	2.15
α_3	−125.4	−0.06	0.52	−120.2	0.02	0.58
α_4	−0.92	−0.52	0.49	−6.37	0.41	0.44
α_5	−382.9	0.11	−0.62	−327.6	0.10	−0.67
α_6	−1336.6	−0.21	−0.72	−1237.8	−0.26	−0.80
α_7	114.2	0.36	0.42	115.4	0.37	0.43
α_8	−557.3	−0.42	0.15	−542.7	−0.56	0.13
α_9	2208.2	−1.45	−0.51	2036.6	−1.62	−0.60

Table 6
Coriolis coupling constants $Z(I, J)$ and Nielsen's centrifugal distortion constants
for ketene

Modes		$ Z(I, J) $		
I	J	Method 1 ^a	Method 2 ^b	Ref. [14]
Coriolis constants (cm ⁻¹)				
X-components				
7	1	0.049	0.051	0.054
7	2	0.055	0.058	0.062
7	3	0.934	0.912	0.949
7	4	0.349	0.403	0.305
8	1	0.773	0.786	0.792
8	2	0.585	0.566	0.560
8	3	0.016	0.028	0.003
8	4	0.244	0.245	0.243
9	1	0.602	0.585	0.577
9	2	0.798	0.811	0.817
9	3	0.017	0.016	0.022
9	4	0.004	0.005	0.003
Y-components				
5	1	0.393	0.502	0.382
5	2	0.602	0.222	0.614
5	3	0.644	0.785	0.653
5	4	0.259	0.288	0.226
6	1	0.348	0.156	—
6	2	0.784	0.962	—
6	3	0.514	0.204	—
6	4	0.012	0.087	—
Z-components				
7	5	0.679	0.848	0.671
7	6	0.545	0.215	0.562
8	5	0.100	0.220	0.098
8	6	0.733	0.695	0.715
9	5	0.727	0.488	0.735
9	6	0.407	0.686	0.417

Nielsen's centrifugal distortion constants (MHz)

D_J	0.003186	0.003042	0.003253
D_{JK}	0.489299	0.547935	0.485300
D_K	21.554	21.154	21.071
R_5	-0.124918	-0.140382	-
$ R_6 \times 10^{-6}$	3.447	3.385	-
$\Delta J \times 10^{-4}$	1.242	1.201	-

^b B97-1/aug-cc-pVTZ//B3LYP/6-31+G**.

neous model are in close agreement with those of East et al. [14] and Duncan et al. [20] from Generalised Harmonic Force Field (GHFF); the average absolute deviation is 0.016. In contrast, the hybrid model gives values with much larger deviation of 0.097. In the case of vibrational modes ν_5 , ν_6 , ν_8 , ν_9 having strong Coriolis coupling, the values of the homogeneous model are particularly closer to the values of these authors than those obtained from the hybrid model. In an exclusive effort, Nemes [24] determined Coriolis constants of ketene by direct spectroscopic analysis and ascertained four Z-components viz., $Z(5, 8)=0.33$, $Z(5, 9)=-0.774$, $Z(6, 8)=0.714$ and $Z(6, 9)=-0.30$. Like East et al. [14] and Duncan et al. [20], our results support their values for $Z(5, 9)$ and $Z(6, 8)$ but are in disagreement with those for $Z(5, 8)$ and $Z(6, 9)$.

Nielsen’s centrifugal distortion constants by homogeneous and hybrid models are also given in Table 6 and compared with the values of East et al. [14]. As in the case of Coriolis coupling constants, the centrifugal distortion constants from homogeneous model are in better agreement with the literature [14] than those from the hybrid model of Barone [7].

4. Conclusions

The present paper reports the main results of a comprehensive study of the vibrational spectrum of ketene computed using second-order perturbation theory treatment based on quartic, cubic and semidiagonal quartic force constants with the density functional theory. The two different models—a homogeneous model using the same density functionals and basis functions for the harmonic calculations and anharmonic corrections and a hybrid model in which the two parts of the calculation are conducted using different density functionals and basis sets, employed in the present calculations, show that the former is superior to the latter in several respects. Hybrid functionals B97-1 give significantly lower errors in frequency and spectroscopic constants than those from B3LYP functionals. A similar conclusion has been drawn by Boese and Martin [4] from their studies on azabenzenes. Both, the homogeneous and hybrid models give similar results for the molecular geometry and the rotational constants in close agreement with the experimental values as well the theoretical values obtained from *ab initio* quartic force field constructed by MP2 and CCSD approaches and augmented for structural optimization by CCSD(T) [14]. The anharmonic frequencies obtained by the second-order perturbative approach are close to the experimental frequencies and do not need any ad hoc scaling that is required in the case of harmonic frequencies. The absolute average error of the fundamental bands is always below 10 cm^{-1} and never exceeds 35 cm^{-1} in the homogeneous model. However, in the hybrid model, the two figures could be as large as 30 and 90 cm^{-1} , respectively. It is also found that in the hybrid model, the B97-1 functionals combined with large basis sets for harmonic frequency calculations provide a set of frequencies which get modified during the anharmonic correction process performed using B3LYP functionals and lower basis sets. Thus during the anharmonic correction process, a new set of harmonic and a corresponding set of anharmonic frequencies are generated. This may be due to reoptimization of the molecular geometry at the lower level during the anharmonic correction. In a similar situation, in the case of the *cis* and *trans* conformers of chlorocarbonyl ketene, we have observed [28] that a combination of harmonic calculations by B97-1/aug-cc-pVTZ and anharmonic corrections by B3LYP/6-31+G** methods yields positive harmonic and anharmonic frequencies for the *trans* conformer but positive harmonic and negative anharmonic frequencies for the *cis* conformer. The above-mentioned inadequacies found in the use of the hybrid model may arise out of one of the following reasons: (a) the basic requirement that the geometry optimization and frequency calculations must be done at the same level of theory to have valid frequencies [27] is not met in the hybrid model; (b) the molecular structure gets reoptimized at the low level for anharmonic corrections; (c) in addition, the perturbation could also diverge for the above reasons, particularly for the very low, very anharmonic terms where the harmonic approximation is not close enough to make the perturbation work. These

inadequacies in the fundamental modes of ketene in the hybrid model are also reflected in the overtones and combination bands where large deviations of up to 180 cm^{-1} from the experimental values are observed. In contrast, the homogeneous model gives values of the overtones and combination bands within a maximum of 35 cm^{-1} of the experimental values. The hybrid model also fails to predict Fermi resonance such as between ν_4 and $2\nu_5$ and gives anharmonicity constants for these modes at variance from the homogeneous model and the literature.

Acknowledgement

A thankful acknowledgement is made of the financial support to this work by the Council of Scientific and Industrial Research (CSIR), New Delhi (India) through a major research project.

References

- [1] A. Miani, E. Cané, P. Palmieri, A. Trombetti, N.C. Handy, J. Chem. Phys. 112 (2000) 248.
- [2] R. Burcl, N.C. Handy, S. Carter, Spectrochim. Acta Part A 59 (2003) 1881.
- [3] V. Barone, Chem. Phys. Lett. 383 (2004) 528.
- [4] A.D. Boese, J.M.L. Martin, J. Phys. Chem. A 108 (2004) 3085.
- [5] V. Barone, J. Phys. Chem. A 108 (2004) 4146.
- [6] V. Barone, G. Festa, A. Grandi, N. Rega, N. Sanna, Chem. Phys. Lett. 388 (2004) 279.
- [7] V. Barone, J. Chem. Phys. 122 (2005) 014108.
- [8] V.P. Gupta, A. Sharma, Spectrochim. Acta Part A 65 (2006) 759.
- [9] W.F. Arendale, W.H. Fletcher, J. Chem. Phys. 24 (1956) 581.
- [10] J. Sheridan, Molecular Spectroscopy (Report of Bologna Meeting), Pergamon Press, New York, 1959, p. 139.
- [11] C.B. Moore, G.C. Pimentel, J. Chem. Phys. 38 (1963) 2816.
- [12] D.M. Smith, J. Chem. Phys. 122 (2005) 034307.
- [13] J.W.C. Johns, J.M.R. Stone, G. Winnewisser, J. Mol. Spectrosc. 42 (1972) 523.
- [14] A.L.L. East, W.D. Allen, S.J. Klippenstein, J. Chem. Phys. 102 (1995) 8506.
- [15] M.J. Frisch, et al., Gaussian 03 W, Gaussian Inc., Wallingford, CT 06092, USA, 2003.
- [16] A. Frisch, A.B. Nielsen, A.J. Holder, GaussView W Version 2, Gaussian Inc., Pittsburgh, PA 151006, USA, 2000.
- [17] M. Gruebele, J.W. Johns, L. Nemes, J. Mol. Spectrosc. 198 (1999) 376.
- [18] A.P. Cox, I.F. Thomas, J. Sheridan, Spectrochim. Acta 15 (1959) 542.
- [19] J.W.C. Johns, L. Nemes, K.M.T. Yamada, T.Y. Wang, J.L. Domenech, J. Santos, P. Cancio, D. Bermejo, J. Ortigoso, R. Escribano, J. Mol. Spectrosc. 156 (1992) 501.
- [20] J.L. Duncan, A.M. Ferguson, J. Harper, K.H. Tonge, F. Hegelund, J. Mol. Spectrosc. 122 (1987) 72.
- [21] P.E.B. Butler, D.R. Eaton, H.W. Thompson, Spectrochim. Acta 13 (1958) 223.
- [22] J.L. Duncan, A.M. Ferguson, Spectrochim. Acta 43A (1987) 1081.
- [23] J.L. Duncan, B. Munro, J. Mol. Spectrosc. 161 (1987) 311.
- [24] L. Nemes, J. Mol. Spectrosc. 72 (1978) 102.
- [25] F. Hegelund, J. Kauppinen, F. Winther, Mol. Phys. 61 (1987) 261.
- [26] H.A. Jahn, Phys. Rev. 56 (1939) 680.
- [27] J.B. Foresman, A. Frisch, Exploring Chemistry with Electronic Structure Methods, Gaussian Inc., 1996.
- [28] V.P. Gupta, unpublished.
- [29] H.R. Johnson, M.W.P. Strandberg, J. Chem. Phys. 20 (1952) 687.